Inorg. Chem. **2008**, *47*, 2039−2048

Synthesis, Separation, and Circularly Polarized Luminescence Studies of Enantiomers of Iridium(III) Luminophores

Frederick J. Coughlin,[†] Michael S. Westrol,[†] Karl D. Oyler,[†] Neal Byrne,[‡] Christina Kraml,[‡] Eli Zysman-Colman,[†] Michael S. Lowry,[†] and Stefan Bernhard*[,†]

Department of Chemistry, Princeton University, Princeton, New Jersey 08544, and Lotus Separations, LLC, 201 Frick Laboratory, Princeton, New Jersey 08544

Received September 5, 2007

A family of heteroleptic $(C\hat{}N)_2Ir(acac)$ and homoleptic *fac*-$Ir(C\hat{}N)_3$ complexes have been synthesized and their photophysical properties studied (where C^N = a substituted 2-phenylpyridine and acac = acetylacetonate). The neutral Δ and Λ complexes were separated with greater than 95% enantiomeric purity by chiral supercritical fluid chromatography, and the solution circular dichroism and circularly polarized luminescence spectra for each of the enantio-enriched iridium complexes were obtained. The experimentally measured emission dissymmetries (g_{em}) for this series compared well with predicted values provided by time-dependent density functional theory calculations. The discovered trend further showed a correlation with the dissymmetries of ionic, enantiopure hemicage compounds of Ru(II) and Zn(II), thus demonstrating the applicability of the model for predicting emission dissymmetry values across a wide range of complexes.

Introduction

Organic light-emitting diodes (OLEDs)[1] incorporating cyclometalated iridium(III) complexes have received increased attention recently.[2–10] These compounds hold particular promise as they are readily color-tuned through systematic modification of the ligands, possess high phosphorescent quantum efficiencies, are photochemically and synthetically stable, and possess a facile synthesis.[11] While racemic mixtures of Ir(III) luminophores emit light with no net polarization, enantio-enriched complexes emit circularly polarized light with a polarization bias. Possible uses for such compounds include three-dimensional electronic displays[12] and biological assays.[13]

Enantiomeric resolution of racemic, bidentate transition metal complexes into their optically active Λ and Δ isomers can be quite difficult and is typically attempted through one of several methods. The most commonly employed technique is cocrystallization with an appropriate chiral counterion;[14] this strategy can be effective for ionic metal complexes but is not conducive for neutral complexes as is the case here. A second means is through synthetic predetermination of the helicity about the metal center, as demonstrated by our group[15] as well as von Zelewsky and co-workers,[16,17] using

* Author to whom correspondence should be addressed. E-mail: bern@princeton.edu.
† Princeton University.
‡ Lotus Separations, LLC.

(1) Hung, L. S.; Chen, C. H. *Mater. Sci. Eng. Rep.* **2002**, 143.
(2) Dixon, I. M.; Collin, J.-P.; Sauvage, J.-P.; Flamigni, L.; Susana, E.; Barigelletti, F. *Chem. Soc. Rev.* **2000**, *29*, 385–391.
(3) Adachi, C.; Baldo, M. A.; Thompson, M. E.; Forrest, S. R. *Appl. Phys.* **2001**, *90*, 5048.
(4) Baldo, M. A.; Lamansky, S.; Burrows, P. E.; Thompson, M. E.; Forrest, S. R. *Appl. Phys. Lett.* **1999**, *75*, 4.
(5) Nazeeruddin, M. K.; Humphry-Baker, R.; Berner, D.; Rivier, S.; Zuppiroli, L.; Grätzel, M. *J. Am. Chem. Soc.* **2003**, *125*, 8790.
(6) Tsuboyama, A.; Iwawaki, H.; Furugori, M.; Mukaide, T.; Kamatani, J.; Igawa, S.; Moriyama, T.; Miura, S.; Takiguchi, T.; Okada, S.; Hoshino, M.; Ueno, K. *J. Am. Chem. Soc.* **2003**, *125*, 12971–12979.
(7) Laskar, I. R.; Hsu, S.-F.; Chen, T.-M. *Polyhedron* **2006**, *25*, 1167–1176.
(8) Hsu, N.-M.; Li, W.-R. *Angew. Chem., Int. Ed.* **2006**, *45*, 4138–4142.
(9) Slinker, J. D.; Gorodetsky, A. A.; Lowry, M. S.; Wang, J. J.; Parker, S.; Rohl, R.; Bernhard, S.; Malliaras, G. G. *J. Am. Chem. Soc.* **2004**, *126*, 2763–2767.
(10) Slinker, J. D.; Koh, C. Y.; Malliaras, G. G.; Lowry, M. S.; Bernhard, S. *Appl. Phys. Lett.* **2005**, *86*, 173506.
(11) Lowry, M. S.; Hudson, W. R.; Pascal, R. A., Jr.; Bernhard, S. *J. Am. Chem. Soc.* **2004**, *126*, 14129–14135.
(12) Lamansky, S.; Djurovich, P.; Murphy, D.; Abdel-Razzaq, F.; Lee, H.-E.; Adachi, C.; Burrows, P. E.; Forrest, S. R.; Thompson, M. E. *J. Am. Chem. Soc.* **2001**, *123*, 4304–4312.
(13) Lo, K. K.-W.; Hui, W.-K.; Chung, C.-K.; Tsang, K. H.-K.; Ng, D. C.-M.; Zhu, N.; Cheung, K.-K. *Coord. Chem. Rev.* **2005**, *249*, 1434–1450.
(14) Sagüés, J. A. A.; Gillard, R. D.; Smalley, D. H.; Williams, P. A. *Inorg. Chim. Acta* **1980**, *43*, 211–216.
(15) Oyler, K. D.; Coughlin, F. J.; Bernhard, S. *J. Am. Chem. Soc.* **2007**, *129*, 210–217.

10.1021/ic701747j CCC: $40.75
Published on Web 02/14/2008

caged, CHIRAGEN-type pineno-polypyridines. Although successful for both ionic and neutral complexes, the generality and applicability of this method is limited as it requires a multistep synthesis of the chiral ligand. Such a process does not lend itself well to systematic studies of subsituent effects for the purposes of excited-state tuning. Finally, chromatographic resolution of Λ and Δ isomers is theoretically possible using a chiral stationary phase but to our knowledge has not been demonstrated or developed for neutral iridium complexes.

When discussing chiral luminescent compounds, a primary property of interest is a complex's emission dissymmetry factor (g_{em}), which indicates the degree to which one type of circularly polarized light (right-handed or left-handed) is preferentially emitted over the other. This value can be measured through circular polarized luminescence (CPL) spectroscopy and is described as the ratio of differential emission intensity (ΔI) to the total intensity (I) in eq 1, where I_L and I_R represent the intensity of left and right circularly polarized luminescence, respectively.

$$g_{em}(\lambda) = \frac{\Delta I}{\frac{1}{2}I} = \frac{I_L - I_R}{\frac{1}{2}(I_L + I_R)} \quad (1)$$

For most practical applications, it is desirable to maximize the absolute value of g_{em} as much as possible in order to produce a signal strong enough to be readily detectable. Typically, values reported in the literature are on the order of 10^{-3} in solution for transition metal complexes.[18–20] Although some lanthanide compounds have exhibited higher emission dissymmetries[21] as a result of their metal-centered f → f transitions, their luminescence is not readily color-tunable, as is the case for certain d-block complexes.

Owing largely to the difficulties associated with enantiomeric resolution along with the lack of commercial CPL spectrometers, little to no work has been conducted to establish any firm relationship or trend between chemical structure and the magnitude of emission dissymmetry, which can subsequently be used as a means to predict the g_{em} value for a given compound. Such a model would serve as a practical tool in the discovery of transition metal complexes possessing both useful luminescent properties and high emission dissymmetry factors. For this reason, we chose to investigate a series of neutral Ir(III) metal complexes by resolving each into its Δ and Λ isomers through chiral chromatography, experimentally measuring their g_{em} factors by CPL, and then using this data to establish a predictable trend in emission dissymmetry using density functional theory (DFT) calculations of the excited state.

For the compounds to be tested, a family of heteroleptic $(C^N)_2Ir(acac)$ and homoleptic *fac*-$Ir(C^N)_3$ complexes were chosen. bis-Cyclometalated iridium complexes containing the β-diketonato ancillary ligand, acac (where acac = acetylacetonate), have been and continue to be an area of great interest. The acac ligand's orbitals have been shown, both computationally and experimentally, to be spectroscopically passive, serving only to affect the ligand field splitting of the complex and thus decrease the highest occupied molecular orbital−lowest unoccupied molecular orbital (HOMO–LUMO) energy gap relative to tris-cyclometalated, homoleptic analogues.[22] Herein, we report the synthesis and enantiomeric separation of this series of six structurally diverse iridium complexes along with their chiroptical properties. Subsequently, computational methods were employed to predict chiroptical absorption (circular dichroism, CD) as well as emission behavior (circular polarized luminescence); these computer simulations were found to agree strongly with the experimental data and provide a heretofore unprecedented means of predicting emission dissymmetry from transition metal complexes.

Experimental Section

General. The syntheses of all ligands and their pyridinium salt precursors have been previously reported[11] with the exception of 3-(4-fluorophenyl)-5,6,7,8-tetrahydroisoquinoline (FCyppy, **1**) and 3-(4-bromophenyl)-5,6,7,8-tetrahydroisoquinoline (BrCyppy, **2**). All solvents and reagents were purchased commercially from either Aldrich or Alfa Aesar and used without any further purification. ^{1}H NMR spectra were recorded on Varian/INOVA 400 and 500 MHz spectrometers. ^{13}C NMR spectra were performed on a Bruker Avance II 500 with TCI cryoprobe with APT spectra processing. Electrospray mass spectra were performed on a Hewlett-Packard 5898B MS Engine. Elemental analysis was carried out by the University of Illinois at Urbana–Champaign Microanalysis Laboratory on an Exeter CE440. HRMS analysis was conducted at the University of Iowa High Resolution Mass Spectrometry Facility.

3-(4-Fluorophenyl)-5,6,7,8-tetrahydroisoquinoline (1). To a solution of 2′-pyridinium bromide-4-fluoroacetophenone (1.51 g, 5.1 mmol, 1 equiv) in 23 mL MeOH was added 1-cyclohexenecarboxaldehyde (680 μL, 5.1 mmol, 1 equiv) and NH_4OAc (2.2 g, 28.5 mmol, 5.6 equiv). The solution was refluxed under N_2 for 20 h. Upon cooling, the reaction was quenched with H_2O and extracted 5× hexanes. The organic layer was washed 2× with H_2O followed by 3× with 2 M HCl, and then the aqueous layer was basified with NaOH (s) and subsequently extracted with 4× hexanes. The organic layer was dried over $MgSO_4$ and filtered through a celite plug. The organic layer was concentrated under reduced pressure then *in vacuo* to yield a light-brown liquid. Yield: 86%. R_f (10% EtOAc/hexanes on silica): 0.28. ^{1}H NMR (500 MHz, $CDCl_3$): δ 8.33 (s, 1H), 7.90 (dd, J = 5.5, 8.5 Hz, 1H), 7.33 (s, 1H), 7.10 (t, J = 8.5 Hz, 2H), 2.77 (m, 4H), 1.82 (m, 4H). ^{13}C NMR (125 MHz, $CDCl_3$): δ 164.1, 162.1, 153.3, 150.2, 146.7, 135.8, 131.6, 128.3, 128.2, 120.3, 115.4, 113.3, 28.9, 25.9, 22.6, 22.4. EI-LRMS calcd for $C_{15}H_{14}FN$: 227.28. Found: 228. Anal. calcd for $C_{15}H_{14}FN$ [M^+]: C, 79.27; H, 6.21; N, 6.16. Found: C, 79.02; H, 6.24; N, 6.23.

(16) Hamann, C.; von Zelewsky, A.; Neels, A.; Stoeckli-Evans, H. *J. Chem. Soc., Dalton Trans.* **2004**, 402–406.
(17) Schaffner-Hamann, C.; von Zelewsky, A.; Barbieri, A.; Barigelletti, F.; Muller, G.; Riehl, J. P.; Neels, A. *J. Am. Chem. Soc.* **2004**, *126*, 9339–9348.
(18) Riehl, J. P.; Richardson, F. S. *Chem. Rev.* **1986**, *86*, 1–16.
(19) Gunde, K. E.; Credi, A.; Jandrasics, E.; von Zelewsky, A.; Richardson, F. S. *Inorg. Chem.* **1997**, *36*, 426–434.
(20) Field, J. E.; Muller, G.; Riehl, J. P.; Venkataraman, D. *J. Am. Chem. Soc.* **2003**, *125*, 11808–11809.
(21) Petoud, S.; Muller, G.; Moore, E. G.; Xu, J.; Sokolnicki, J.; Riehl, J. P.; Le, U. N.; Cohen, S. M.; Raymond, K. N. *J. Am. Chem. Soc.* **2007**, *129*, 77–83.
(22) Ragni, R.; Plummer, E. A.; Brunner, K.; Hofstraat, J. W.; Babudri, F.; Farinola, G. M.; Naso, F.; De Cola, L. *J. Mater. Chem.* **2006**, *16*, 1161–1170.

3-(4-Bromophenyl)-5,6,7,8-tetrahydroisoquinoline (2). To a solution of 2′-pyridinium bromide-4-bromoacetophenone (10.6 g, 29.6 mmol, 1 equiv) in 100 mL of MeOH was added 1-cyclohexenecarboxaldehyde (3.4 mL, 31.2 mmol, 1.05 equiv) and NH_4OAc (10.8 g, 140.3 mmol, 4.7 equiv). The solution was refluxed under N_2 for 20 h. Upon cooling, the red-colored reaction was quenched with H_2O. The tan precipitate was filtered through a Buchner funnel and washed copiously with H_2O. The tan solid was dried under reduced pressure then *in vacuo* to yield a light-tan solid. Yield: 76%. R_f (10% EtOAc/hexanes on silica): 0.35. ^{1}H NMR (500 MHz, $CDCl_3$): δ 8.33 (s, 1H), 7.79 (d, J = 8.8 Hz, 1H), 7.53 (d, J = 8.8 Hz, 2H), 7.34 (s, 1H), 2.76 (m, 4H), 1.81 (m, 4H). ^{13}C NMR (125 MHz, $CDCl_3$): δ 153.0, 150.2, 146.8, 138.5, 132.0, 131.6, 128.1, 122.6, 120.3, 28.8, 26.0, 22.5, 22.3. EI-LRMS calcd for $C_{15}H_{14}BrN$ [M^+]: 288.19. Found: 287.0. Anal. calcd for $C_{15}H_{14}BrN$: C, 62.52; H, 4.90; N, 4.86. Found: C, 62.20; H, 4.89, N 4.91.

Synthesis of Tetrakis-(C^N)-μ-(dichloro)-diiridium(III). The syntheses of the ligands[11] and chloro-bridged dimers have been reported previously.[11,12,23] The $IrCl_3 \cdot nH_2O$ is combined with 2.1 equiv of cyclometalating ligand (C^N) in a 3:1 mixture of 2-methoxyethanol and water. The reaction was heated to 125 °C for 18 h. Upon cooling, the reaction was quenched with H_2O. The precipitate was isolated by vacuum filtration through a Buchner funnel and washed copiously with water and hexanes. The yellow solid was vaccuum-dried to yield the product, $[(C^N)_2Ir\text{-}\mu\text{-}Cl]_2$. Yield: 70–85%.

Synthesis of bis-(C^N)-(Acetylacetonato)-iridium(III) Complexes. The synthesis of each complex was performed on the basis of a previously reported procedure.[5] To a solution of corresponding dimer (0.03 mmol, 1 equiv) in 5 mL of CH_2Cl_2 was added acetylacetone (8.23 μL, 0.08 mmol, 2.7 equiv) in 0.5 mL of EtOH. To this mixture was added tetrabutylammonium hydroxide as a 40% w/w aqueous solution (53 μL, 0.51 mmol, 16.9 equiv). The reaction mixture was refluxed for 18 h. Upon cooling, the crude mixture was run through a short silica plug using CH_2Cl_2 as the eluent to remove baseline impurities. The yellow solution was then concentrated 90%, and ca. 2 mL of EtOH was added. The remaining CH_2Cl_2 was removed under reduced pressure to form a yellow crystalline precipitate. The EtOH suspension was then cooled in an ice bath for 10 min to promote additional crystallization. The solid was collected by vacuum filtration through a Buchner funnel, washed with cold EtOH, and vaccuum-dried to yield the desired heteroleptic $(C^N)_2Ir(acac)$ product. Yield: 80–90%.

$(ppy)_2Ir(acac)$ (3) (ppy = 2-phenylpyridine)[23]. ^{1}H NMR (400 MHz, $CDCl_3$): δ 8.47 (d, J = 6.0 Hz, 2H), 7.80 (d, J = 8.0 Hz, 2H), 7.68 (t, J = 7.6 Hz, 2H,), 7.50 (d, J = 7.6 Hz, 2H), 7.09 (t, J = 7.6 Hz, 2H), 6.76 (t, J = 7.6 Hz, 2H), 6.64 (t, J = 7.6 Hz, 2H), 6.22 (d, J = 7.6 Hz, 2H), 5.17 (s, 1H), 1.74 (s, 6H).

$(Fmppy)_2Ir(acac)$ (4). ^{1}H NMR (500 MHz, $CDCl_3$): δ 8.23 (s, 2H), 7.65 (d, J = 8.2 Hz, 2H), 7.53 (d, J = 8.2 Hz, 2H), 7.45 (dd, J = 8.2 Hz, J_{HF} = 6.1 Hz, 2H), 6.50 (dd, J = 8.6 Hz, J_{HF} = 7.0 Hz, 2H), 5.82 (d, J_{HF} = 9.8 Hz, 2H), 5.22 (s, 1H), 2.38 (s, 6H), 1.79 (s, 6H). ^{13}C NMR (125 MHz, $CDCl_3$): δ 184.71, 164.86, 161.56, 149.45, 147.77, 141.17, 138.08, 131.17, 124.83, 119.02, 118.01, 108.00, 100.63, 28.84, 18.52. ESI-LRMS calcd for $C_{24}H_{17}F_2IrN_2$[M^+ - $C_5H_8O_2$]: 563.62. Found: 564. Anal. calcd for $C_{29}H_{25}F_2IrN_2O_2$: C, 52.48; H, 3.80; N, 4.22. Found: C, 51.96; H, 3.83; N, 4.25.

$(MeOmppy)_2Ir(acac)$ (5). ^{1}H NMR (400 MHz, $CDCl_3$): δ 8.22 (s, 2H), 7.58 (d, J = 8.4 Hz, 2H), 7.46 (dd, J = 1.6, 8.4 Hz, 2H), 7.41 (d, J = 8.4 Hz, 2H), 6.35 (dd, J = 2.8, 8.8 Hz, 2H), 5.73 (d, J = 2.4 Hz, 2H), 5.18 (s, 1H), 3.52 (s, 6H), 2.34 (s, 6H), 1.77 (s, 6H). ^{13}C NMR (125 MHz, $CDCl_3$): δ 184.43, 165.61, 159.29, 148.70, 147.66, 138.29, 137.55, 129.78, 124.51, 118.34, 117.25, 105.78, 100.45, 54.43, 28.88, 18.45. ESI-LRMS calcd for $C_{26}H_{23}IrN_2O_2$ [M^+ - $C_5H_8O_2$]: 587.7. Found: 588. Anal. calcd for $C_{31}H_{31}IrN_2O_4 \cdot 2H_2O$: C, 51.44; H, 4.87; N, 3.87. Found: C, 51.63; H, 4.57; N, 3.85.

$(Phmppy)_2Ir(acac)$ (6). ^{1}H NMR (400 MHz, $CDCl_3$): δ 8.34 (s, 2H), 7.75 (d, J = 8.0 Hz, 2H), 7.54 (dd, J = 2.0, 8.4 Hz, 2H), 7.53 (d, J = 8.0 Hz, 2H), 7.29 (m, 4H), 7.24 (m, 4H), 7.17 (m, 2H), 7.00 (dd, J = 2.0, 8.0 Hz, 2H), 6.44 (d, J = 1.6 Hz, 2H), 5.21 (s, 1H), 2.39 (s, 6H), 1.80 (s, 6H). ^{13}C NMR (125 MHz, $CDCl_3$): δ 184.52, 165.66, 148.02, 146.84, 144.51, 142.05, 140.48, 137.65, 131.46, 131.02, 128.22, 127.21, 127.14, 126.51, 123.48, 120.10, 118.06, 28.91, 18.59. ESI-LRMS calcd for $C_{38}H_{30}IrN_2O$ [M^+ - C_3H_5O]: 722.89. Found: 723. Anal. calcd for $C_{41}H_{35}IrN_2O_2 \cdot H_2O$: C, 61.71; H, 4.67; N, 3.51. Found: C, 61.35; H, 4.62; N, 3.71.

$(BrCyppy)_2Ir(acac)$ (7). ^{1}H NMR (400 MHz, $CDCl_3$): δ 8.04 (s, 2H), 7.46 (s, 2H), 7.30 (d, J = 8.4 Hz, 2H), 6.92 (dd, J = 2.0, 8.4 Hz, 2H), 6.28 (d, J = 2.0 Hz, 2H), 5.17 (s, 1H), 2.99 (m, 4H), 2.76 (m, 4H), 1.88 (m, 8H), 1.76 (s, 6H). ^{13}C NMR (125 MHz, CD_2Cl_2): δ 184.97, 163.46, 149.04, 149.02, 148.31, 145.27, 135.59, 132.95, 124.67, 124.26, 122.81, 119.29, 100.81, 29.41, 28.76, 26.76, 22.67, 22.62. ESI-LRMS calcd for $C_{32}H_{28}Br_2IrN_2O$ [M^+ - C_3H_5O]: 808.61. Found: 808. Anal. calcd for $C_{35}H_{33}Br_2IrN_2O_2$: C, 48.56; H, 3.84; N, 3.24. Found: C, 48.59; H, 4.27; N, 3.25.

$(dFmppy)_2Ir(acac)$ (8). ^{1}H NMR (300 MHz, $CDCl_3$): δ 8.23 (s, 2H), 8.13 (d, J = 8.5 Hz, 2H), 7.60 (d, J = 8.26 Hz, 2H), 6.31 (ddd, J = 2.4, 6.9, 9.3 Hz, 2H), 5.62 (d, J = 9.1 Hz, 2H), 5.25 (s, 1H), 2.41 (s, 6H), 1.82 (s, 6H). ^{13}C NMR (125 MHz, CDCl3): δ 184.88, 163.22, 162.54, 150.40, 147.75, 138.63, 137.76, 131.52, 128.70, 122.15, 114.90, 100.77, 97.19, 28.83, 18.56. ESI-LRMS calcd for $C_{24}H_{15}F_4IrN_2$ [M^+ - $C_5H_8O_2$]: 599.61. Found: 599.

$(dF(CF_3)ppy)_2Ir(acac)$ (9). ^{1}H NMR (400 MHz, $CDCl_3$): δ 8.63 (s, 2H), 8.34 (dd, J = 2.0, 8.4 Hz, 2H), 7.98 (dd, J = 2.4, 8.8 Hz, 2H), 6.70 (m, 2H), 5.61 (dd, J = 2.0, 8.4 Hz, 2H), 5.29 (s, 1H), 1.81 (s, 6H). ^{13}C NMR (125 MHz, $CDCl_3$): δ 185.80, 168.63, 162.70, 160.87, 152.40, 144.92, 135.30, 127.30, 124.21, 122.27, 121.41, 115.46, 101.17, 98.04, 28.57. ESI-LRMS calcd for $C_{29}H_{17}F_{10}IrN_2O_2$ [M^+]: 807.67. Found: 806. ESI-LRMS calcd for $C_{24}H_9F_{10}IrN_2$ [M^+ - $C_5H_8O_2$]: 707.553. Found: 706.

Synthesis of *fac*-Ir(C^N)$_3$ Complexes. A solution of $Ir(acac)_3$ (100 mg, 0.25 mmol, 1 equiv) and the C^N ligand (0.77 mmol, 3.1 equiv) in 4 mL of ethylene glycol was heated to 250 °C for 42 h under a stream of N_2. Upon cooling, the reaction was diluted with H_2O and CH_2Cl_2. The aqueous phase was extracted 4× with CH_2Cl_2. The organic phase was concentrated under reduced pressure and then purified via flash column chromatography (CH_2Cl_2 on silica) to yield the desired product.

***fac*-Ir(FCyppy)$_3$ (10).** Yield: 83%. R_f (CH_2Cl_2 on silica): 0.73. ^{1}H NMR (400 MHz, $CDCl_3$): δ 7.50 (dd, J = 5.6, 8.8 Hz, 1H), 7.43 (s, 1H), 7.14 (s, 1H), 6.53 (dt, J = 2.8, 8.8 Hz, 1H), 6.35 (dd, J = 2.8, 10.4 Hz, 1H), 2.80 (m, 2H), 2.45 (m, 2H), 1.71 (m, 4H). ^{13}C NMR (100 MHz, $CDCl_3$): δ 164.8, 163.2, 162.1, 146.8, 146.6, 140.3, 131.2, 124.6, 124.5, 122.1, 121.9, 118.5, 107.1, 106.8, 28.9, 26.2, 22.3, 22.2. EI-LRMS calcd for $C_{45}H_{39}F_3IrN_3$ [M^+]: 871.038. Found: 873.0. EI-HRMS for $C_{45}H_{39}F_3{}^{191}IrN_3$: 869.273. Found: 869.270.

***fac*-Ir(BrCyppy)$_3$ (11).** Yield: 80%. R_f (CH_2Cl_2 on silica): 0.81. ^{1}H NMR (500 MHz, $CDCl_3$): δ 7.47 (s, 1H), 7.38 (d, J = 8.5 Hz, 1H), 7.08 (s, 1H), 6.98 (d, J = 8.5 Hz, 1H), 6.76 (s, 1H), 2.82 (m, 2H), 2.43 (m, 2H), 1.72 (m, 4H). ^{13}C NMR (125 MHz, $CDCl_3$): δ

(23) Lamansky, S.; Djurovich, P.; Murphy, D.; Abdel-Razzaq, F.; Kwong, R.; Tsyba, I.; Bortz, M.; Mui, B.; Bau, R.; Thompson, M. E. *Inorg. Chem.* **2001**, *40*, 1704–1711.

162.2, 146.9, 146.8, 143.1, 138.7, 131.9, 124.7, 124.5, 123.1, 118.9, 100.0, 29.0, 26.2, 22.3, 22.2. EI-LRMS calcd for $C_{45}H_{42}Br_3IrN_3[M^+]$: 1056.78. Found: 1054.0. Anal. calcd for $C_{45}H_{42}Br_3IrN_3 \cdot 4H_2O$: C, 48.01; H, 4.21; N, 3.73. Found: C, 47.71; H, 3.82, N 3.65.

Enantiomeric Separation. 1. Analytical Supercritical Fluid Chromatography (SFC) Separations. Samples were analyzed on a Berger Analytical SFC System equipped with a dual pump (FCM-1200), an auto sampler (ALS 3100), a column oven (TCM-200), and a diode-array detector (DAD-4100) (Berger Instruments, Newark, DE). Analyses were carried out on a Chiralpak AD-H (0.46 × 25 cm) column under isocratic conditions using 30% or 40% of the organic modifier (methanol or ethanol) in CO_2 at a back pressure of 100 bar with a flow rate of 3 mL/min and temperature of 40 °C.

2. Preparative SFC Separations. Separations were carried out on a Berger Multigram II SFC equipped with two SD-1 Varian pumps and a Knauer K-2501 Spectrophotometer (Mettler-Toledo, Newark, DE). Samples were dissolved to an approximate concentration of 0.1 mg/mL in ethanol/dichloromethane. A total of 1 mL of solution was injected at intervals of 60 s onto a (2 × 15 cm) Chiralpak AD-H column under isocratic conditions using 30% or 40% of the organic modifier (methanol or ethanol) in CO_2 at a back pressure of 100 bar with a flow rate of 50 mL/min and temperature of 35 °C. Sample peaks were acquired using collection "windows" at a wavelength of 280 nm.

Photophysical Characterization. UV–vis spectra were recorded at room temperature in a 1.0 cm quartz cuvette using a Hewlett-Packard 8453 spectrometer equipped with a diode-array detector. The samples were prepared in toluene at a concentration of 25 μM, with the exception of the ruthenium standard ($[Ru(bpy)_3](PF_6)_2$), which was prepared in acetonitrile.

Emission spectra were recorded using a Jobin-Yvon Fluorolog-3 spectrometer equipped with a double monochromator and a Hamamatsu-928 photomultiplier tube (PMT) as the detector. Right angle detection was used for the complexes, which were all excited at 400 nm.

Excited-state lifetimes were measured using the emission monochromator and PMT detector of the Jobin-Yvon Fluorolog-3 spectrometer. The samples were excited at 337 nm with a N_2 laser (Laser Science, Inc. VSL-337LRF, 10 ns pulse), and the emission decay was recorded using a Tektronix TDS 3032B digital phosphor oscilloscope. All samples were degassed using N_2 for 10 min prior to measurements.

Chiroptical Characterization. Upon receiving the resolved enantiomers from the chiral SFC separation, chiroptical measurements were performed. Solutions were made using toluene at concentrations of 25 μM for the purposes of CD and CPL analysis. CD measurements were performed on an AVIV-62DS spectrometer with a 1.0 cm path length. Data points were collected at 1 nm intervals using averaging times of 1 s/nm with a spectral bandwidth of 1.5 nm.

The CPL measurements were performed as follows: The emission of the samples was detected at a 90° angle to the excitation in a Jobin-Yvon Fluorolog-3 and was passed through a photoelastic modulator (Hinds International PEM-90, operating at a modulation frequency of 50 kHz), followed by a linear polarizer. The light was then incident upon the emission monochromator. A Hamamatsu-928 PMT in conjunction with a gated photon counter (Stanford Research SR 400) was used to acquire the CPL spectrum.[24] To ensure that there was no bias toward one type of circularly polarized light, a solution containing a racemic mixture of bipyridyl hemicage complex $[Ru(\mathbf{L_3})](PF_6)_2$[15] was measured. A slight bias was found, as the average value of g_{em} was -7.9×10^{-5}. To adjust for this, ΔI for all CPL measurements was corrected using eq 2.

$$\Delta I_{corr} = \Delta I_{exp} + \frac{7.9 \times 10^{-5}}{2} I_{exp} \quad (2)$$

Computational Methodology. All DFT calculations were carried out with the Gaussian 03 suite.[25] Ground-state and excited-state geometries (both singlet and triplet) for all complexes were evaluated computationally using Becke's three-parameter exchange functional (B3)[26] in conjunction with the Lee, Yang, and Parr (LYP)[27,28] nonlocal functional using the default thresholds for gradient convergence but with a slightly relaxed threshold for wave function convergence [SCF=(CONVER=7)]. The LANL2DZ basis set was employed for all calculations.[29–31] For each complex, time-dependent DFT (TD-DFT) calculations were performed at the optimized ground-state geometry, calculating the energy, oscillator strength, and rotatory strength for each of the 100 lowest singlet excitations. The geometry of the lowest triplet state was also obtained using unrestricted B3LYP calculations, and the energy difference between the singlet and triplet states was calculated at this geometry. Prediction of CD spectra was accomplished using GaussSum 2.0.[32] Electronic transitions were expanded as Gaussian curves, with a full-width at half-maximum (fwhm) for each peak set to 0.12 eV.

Results and Discussion

Synthesis of Iridium Complexes. The free ligands were accessed via the Kröhnke condensation[33] reaction from the corresponding substituted phenacylpyridinium bromide, enal, and ammonium acetate. The cyclohexyl-fused ppy ligands present in complexes **7**, **10**, and **11** were chosen to both increase solubility and extend the helicity of the complexes and enhance their interaction with the chiral stationary phase in the SFC separation. The heteroleptic complexes, $(C\hat{}N)_2Ir(acac)$, were synthesized through a sequential two-step procedure (Scheme 1, top). Dimer formation occurred readily, the product of which precipitated out of the reaction. The chloride-bridged iridium dimer was then cleaved under basic conditions (TBAOH) to form the desired complexes **3–9** (Scheme 1, bottom) in good yield.[5] Removal of polymeric side products through a short silica plug followed by precipitation with cold ethanol resulted in pure heteroleptic iridium complexes.

The preparation of the corresponding homoleptic *fac*-$Ir(C\hat{}N)_3$ complexes **10** and **11** occurred in excellent yield under a modified literature[34] procedure using ethylene glycol as the solvent. Good conversion was possible with the

(24) Schippers, P. H.; van den Beukel, A.; Dekkers, H. P. J. M. *J. Phys. E: Sci. Instrum.* **1982**, *15*, 945–950.

(25) Frisch, M. J. et al. *Gaussian 03*, revision C.02; Gaussian Inc.: Wallingford, CT, 2004 (see Supporting Information for full citation).
(26) Becke, A. D. *J. Chem. Phys.* **1993**, *98*, 5648–5652.
(27) Lee, C.; Yang, W.; Parr, R. G. *Phys. Rev. B: Condens. Matter Mater. Phys.* **1988**, *37*, 785–789.
(28) Miehlich, B.; Savin, A.; Stoll, H.; Preuss, H. *Chem. Phys. Lett.* **1989**, *157*, 200.
(29) Hay, P. J.; Wadt, W. R. *J. Chem. Phys.* **1985**, *82*, 299–310.
(30) Hay, P. J.; Wadt, W. R. *J. Chem. Phys.* **1985**, *82*, 270–283.
(31) Wadt, W. R.; Hay, P. J. *J. Chem. Phys.* **1985**, *82*, 284–298.
(32) O'Boyle, N. M. *GaussSum 2.0*; Dublin City University: Dublin Ireland, 2006. Available at http://gausssum.sf.net.
(33) Kröhnke, F. *Synthesis* **1976**, 1.
(34) Dedeian, K.; Djurovich, P. I.; Garces, F. O.; Carlson, G.; Watts, R. J. *Inorg. Chem.* **1991**, *30*, 1685–1687.

Scheme 1. (Top) General Synthesis of Heteroleptic $(C^N)_2Ir(acac)$ Complexes Using **3** as an Example[a,b] and (Bottom) Structures of All Ir(III) Complexes Synthesized, Including Homoleptic **10** and **11**

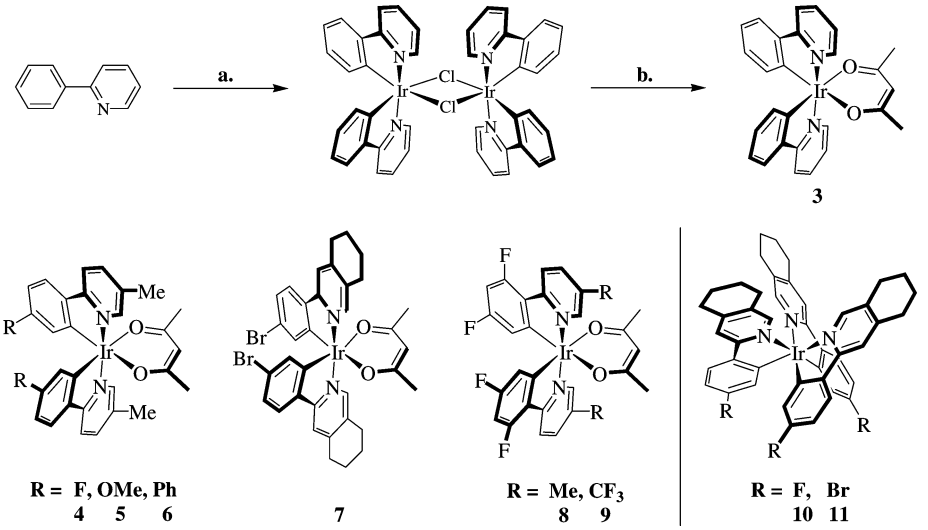

[a] $IrCl_3$/3:1 2-methoxyethanol/water, 125 °C, 18 h. [b] Acetylacetone (acacH)/10:1 CH_2Cl_2/EtOH, TBAOH, reflux, 18 h; TBAOH = *tert*-butylammonium hydroxide.

presence of electron-withdrawing groups on the phenyl ring (Br, F) *para* to the pyridine. Their presence facilitates C−H activation in the cyclometalation of the substituted ppy (2-phenylpyridine) ligands. The facial homoleptic complexes were formed exclusively, as indicated by SFC and ^{1}H NMR, which showed magnetically equivalent phenylpyridines, an indication of the C_3 symmetry of the complex.

Enantiomeric Separation. Iridium complexes (**3**–**7** and **10**) were readily resolved on chiral stationary phases (specifically the amylose-based Chiralpak AD-H columns) using SFC. The characteristically low solubility of these compounds in the mobile phases, consisting of supercritical carbon dioxide mixed with 30−40% methanol or ethanol, resulted in relatively low throughputs. Nonetheless, employing an iterative approach, milligram quantities (up to 200 mg) were resolved using a Multigram II Berger SFC system. Automated "stacked" injections and collections, as well as the addition of 5% dichloromethane to the mobile phase were required to generate sufficient quantities of the desired enantiomers, with enantiomeric excesses (ee) ranging from 95 to 100% (Figure 1). Not all complexes could be resolved in this manner. For instance, highly electron-deficient $(dFmppy)_2Ir(acac)$ (**8**) could not interact sufficiently with the chiral stationary phase to enable enantiomeric separation, while *fac*-$Ir(BrCyppy)_3$ (**11**) proved too insoluble to effectively load onto the column using the devised eluent conditions, despite the presence of the solubility-enhancing cyclohexyl ring. Of the nine iridium (III) complexes synthesized, six (**3**–**7** and **10**) could be separated by SFC and chiroptically analyzed.

Photophysical Observations. Spectroscopic data for the six complexes that were successfully resolved into their separate enantiomers are summarized in Table 1. The UV–vis absorption spectra closely resemble those of typical bis-cyclometalated Ir(III) acac complexes. Intense bands belonging to spin-allowed, singlet ligand-centered (^{1}LC) transitions localized on the phenylpyridine ligands are visible in the UV

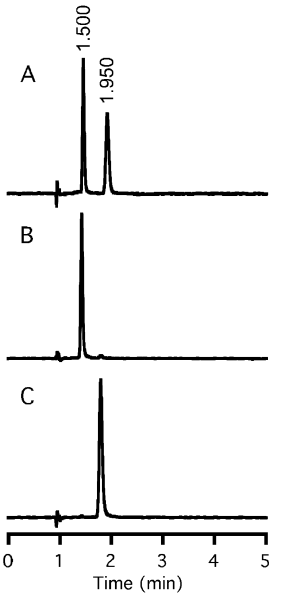

Figure 1. Representative chromatogram for **5**. Chiralpak AD-H (0.46 × 25 cm), 40% ethanol in CO_2 (100 bar), 3 mL/min, 280 nm. (A) Racemic mixture of **5**. (B) Isolated Λ enantiomer peak 1 (ee > 99%). (C) Isolated Δ enantiomer peak 2 (ee > 99%).

region, while much lower intensity bands are present between 372 and 411 nm and 427 and 480 nm, which likely correspond to mostly spin-allowed singlet metal-to-ligand charge-transfer (^{1}MLCT) transitions and spin-forbidden ^{3}MLCT transitions, respectively.[7] These bands may also be partially associated with ligand-centered transitions, as well.[35] These transitions are clearly resolved in the $(C^N)_2Ir(acac)$ series but are not as readily distinguished for the two $Ir(C^N)_3$ complexes. The relatively high intensity of the more red-shifted, spin-forbidden ^{3}MLCT bands compared to the ^{1}MLCT bands is an indication of the large extent of

(35) Wu, F.-I.; Su, H.-J.; Shu, C.-F.; Luo, L.; Diau, W.-G.; Cheng, C.-H.; Jiun-Pey, D.; Lee, G.-H. *J. Mater. Chem.* **2005**, *15*, 1035–1042.

Table 1. Photophysical Data for Chromatographically Resolvable Ir(III) Complexes[a,b,c]

Complex	Ligand (C^N)	Absorption	Emission		
		λ (nm), (log ε)	λ_{max} (nm)	τ (μs)	Φ_{PL}
(C^N)$_2$Ir(acac):					
ppy - **3**	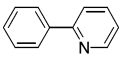	341 (4.0), 411 (3.5), 464 (3.4)	516	1.68	0.36
Fmppy - **4**	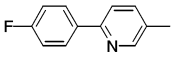	353 (3.9), 397 (3.7), 480 (2.7)	490	1.43	0.28
MeOmppy - **5**	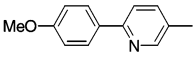	362 (4.0), 404 (3.7), 434 (3.6)	501	1.67	0.31
Phmppy - **6**	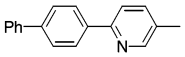	314 (4.6), 372 (3.9), 427 (3.6)	537	3.06	0.30
BrCyppy - **7**	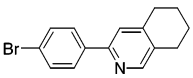	333 (4.0), 400 (3.6), 435 (3.4)	492	1.84	0.28
Ir(C^N)$_3$:					
FCyppy - **10**	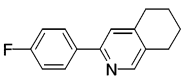	346 (4.0), 388 (3.7), 463 (2.4)	471	1.94	0.34

[a] Measured in N_2-saturated toluene solvent at 25 °C. [b] ε, Φ, and τ are ±10% or better. [c] The emission quantum yields (Φ_{PL}) were measured vs $[Ru(bpy)_3](PF_6)_2$ ($\Phi_{PL} = 0.062$).

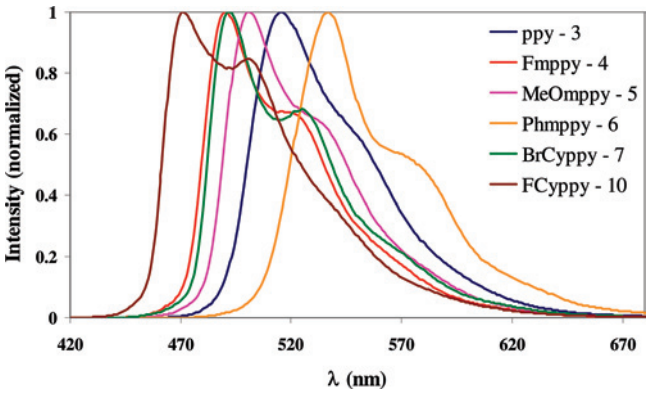

Figure 2. Normalized emission spectra of the Ir(III) complexes **3**–**7** and **10**. The solutions were 25 μM in toluene.

spin–orbit coupling present in these complexes, as previous studies of similar compounds have also shown.[12,23,35]

Normalized room-temperature emission spectra of the complexes are depicted in Figure 2. The emission ranges from blue to green, with Ir(FCyppy)$_3$ (**10**) possessing the highest energy light at 471 nm and (Phmppy)$_2$Ir(acac) (**6**) possessing the lowest at 537 nm; the former is hypsochromically shifted change due to the inductive effects of fluorine substitution, while the latter is bathochromically shifted as a result of the extended π network found on the phenylpyridine ligands. Replacement of one of the phenylpyridine ligands for an acac bathochromically shifts the emission spectrum by ca. 20 nm (**10** vs **4**). With the exception of (ppy)$_2$Ir(acac) (**3**), whose emission spectrum is relatively broad and featureless (an indication of predominant ^{3}MLCT character), the emission spectra of the remaining iridium complexes possess multiple discernible transitions, suggesting the presence of significant ^{3}LC character. Indeed, cyclometalated iridium compounds have been well-documented to emit from a mixed excited state, displaying characteristics of both ^{3}LC and ^{3}MLCT emission.[12]

The emission quantum yields in degassed toluene solutions excited at 400 nm, ranging from 0.28 to 0.36, are similar to those previously reported in 2-methyltetrahydrofuran for analogous (C^N)$_2$Ir(acac) complexes.[12,36] Lifetime measurements for the majority of the complexes ranged from 1 to 2 μs, which is also consistent with data collected for similar neutral Ir(III) compounds.[12,23] DFT calculations suggest that the longer lifetime (3.08 μs) observed for (Phmppy)$_2$Ir(acac) (**6**) results from less probable relaxation from the more twisted excited-state conformation ($\varphi_{biphenyl} = 30°$) of the biphenyl moiety to that of the ground state ($\varphi_{biphenyl} = 20°$).

Chiroptical Characterization. The CD spectra of the enantiomers of **5** are representative of the series of neutral iridium complexes and are depicted in Figure 3 (the spectra of **3**–**7** and **10** are reported in the Supporting Information). From the selected spectra of **5**, it is evident that each resolved species absorbs essentially opposite polarization but with equal intensity.

The CPL analysis further supports the clean resolution of the two enantiomeric complexes by chiral SFC. Like the CD spectra, the two peaks exhibit a "handedness" for the polarization of the emitted light. The CPL spectra for **5** (Figure 4A) shows the characteristic symmetry indicative of

(36) Li, J.; Djurovich, P. I.; Alleyne, B. D.; Yousufuddin, M.; Ho, N. N.; Thomas, J. C.; Peters, J. C.; Bau, R.; Thompson, M. E. *Inorg. Chem.* **2005**, *44*, 1713–1727.

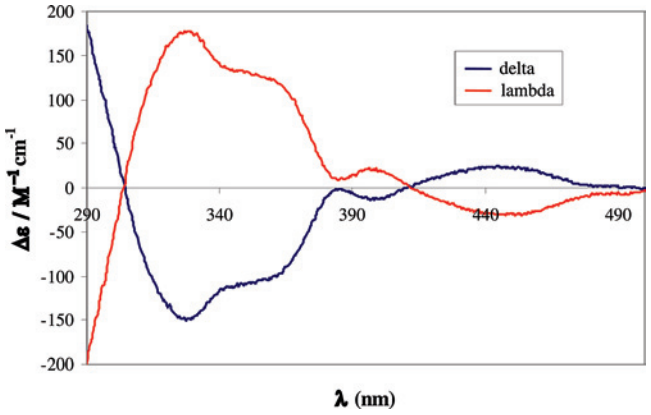

Figure 3. CD spectra for the resolved enantiomers of **5**. The solutions were 25 μM in toluene.

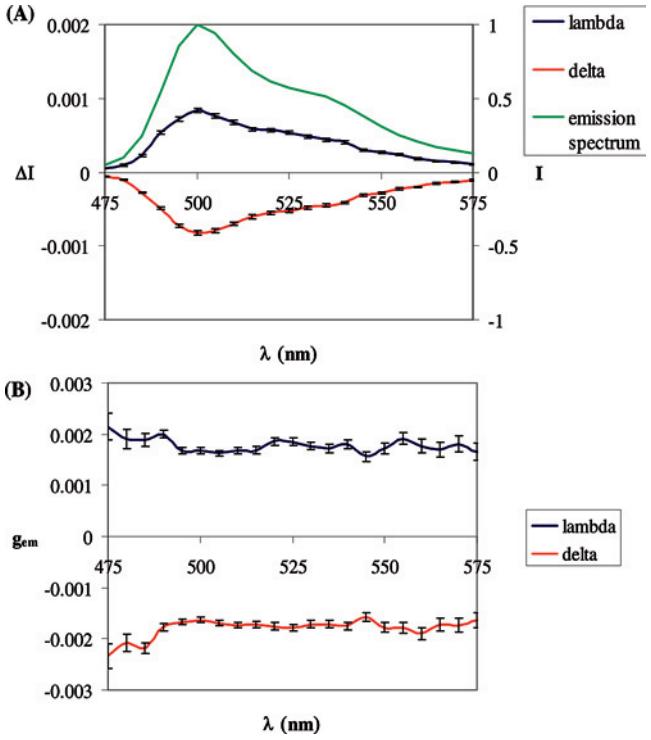

Figure 4. (A) Total emission and CPL spectra of **5**. (B) Emission dissymmetry (g_{em}) of **5** as a function of wavelength.

a predominance of either Δ or Λ isomerism. As the spectrophotometer setup was designed to only detect circularly polarized light, an achiral or racemic sample would not display a signal, as it would have no directional preference for emitting circularly polarized light.

Figure 4B depicts the determined emission dissymmetry value (g_{em}) for **5** as a function of wavelength. The overall g_{em} values in solution are on the order of 10^{-3} (Table 2) and are generally above average for typical transition metal luminophores.[18–20] Among the acac complexes, the g_{em} ranges from 4.7×10^{-4} for the (Phmppy)$_2$Ir(acac) (**6**) to 1.72×10^{-3} for (MeOmppy)$_2$Ir(acac) (**5**). We report g_{em} at $\lambda_{½}$, which is defined as the wavelength at which half the area under the emission curve has been integrated, in order to account for vibrational effects present in the luminescence spectrum. In this manner, g_{em} at $\lambda_{½}$ represents a more accurate depiction of a complex's ability to emit one direction of circularly polarized light as compared to g_{em} determined at λ_{max}.

Table 2. Emission Dissymmetry Data

complex	$\lambda_{½}$ (nm)[a]	g_{em} at $\lambda_{½}$ ($\times 10^{-3}$)
Λ-(ppy)$_2$Ir(acac) - **3**	525	+0.78
Λ-(Fmppy)$_2$Ir(acac) - **4**	505	+1.51
Λ-(MeOmppy)$_2$Ir(acac) - **5**	515	+1.72
Λ-(Phmppy)$_2$Ir(acac) - **6**	545	+0.60
Λ-(BrCyppy)$_2$Ir(acac) - **7**	510	+0.57
Λ-Ir(FCyppy)$_3$- **10**	495	+1.99
Λ-Zn(hemicage)[15]	450	+2.70
Λ-Ru(hemicage)[15]	610	+0.61

[a] $\lambda_{½}$ is defined as the wavelength at which the geometric centroid occurs (see text).

Emission dissymmetry values are influenced by the structure of the complexes. Compounds incorporating greater helical twists should exhibit larger g_{em} values by providing a circular path for electron flow. This may explain the relatively larger value (1.99×10^{-3}) found for **10**, which possesses C_3 symmetry, as compared to the (C^N)$_2$Ir(acac) complexes, which are C_2 symmetric. Introduction of conformational flexibility may result in a lower g_{em} value (**6** and **7**) in complexes of low symmetry, while the inclusion of electron-donating or electron-withdrawing groups at the 4 position of the phenylpyridine ligand results in an increased g_{em} value (**4** or **5** vs **3**).

Computational Modeling. 1. Circular Dichroism. TD-DFT methods are an established means of effectively predicting CD spectra for metal complexes.[37–40] This can be conducted through the determination of the difference in absorptivity of right and left circularly polarized light ($\Delta\epsilon$) from the singlet transitions at a given wavelength, λ (eq 3):

$$\Delta\epsilon(\lambda) = \frac{1}{2.297 \times 10^{-39} \times \sqrt{2\pi\sigma}} \sum_{i}^{A} E_i R_i \, e^{-\left[\frac{(\lambda - E_i)}{2\sigma}\right]^2} \quad (3)$$

where E_i is the energy of the ith transition, R_i is the rotatory strength, and σ is the line width (fwhm) of the absorption band.[41]

TD-DFT-based predictions of the CD spectra were applied to each of the resolved Ir(III) complexes and compared to the experimental measurements. For the calculations, the Λ geometry was applied, and a representative comparison of the simulated and experimental CD spectra of **5** is shown in Figure 5 (simulations of the remaining complexes are found in the Supporting Information). Each CD spectrum consists of two regions: a weak, low-energy, mixed ^{1}LC−^{1}MLCT transition associated with the metal ion as well as the π and π^* orbitals of the C^N ligands, and the more intense, higher-energy ^{1}LC absorptions located exclusively on the C^N ligands. The orbitals involved in the former transition are shown in Figure 6 for complex **5**. All of the simulations show very good agreement to experimental measurements with

(37) Jorge, F. E.; Autschbach, J.; Ziegler, T. *J. Am. Chem. Soc.* **2005**, *127*, 975–985.
(38) Autschbach, J.; Jorge, F. E.; Ziegler, T. *Inorg. Chem.* **2003**, *42*, 2867–2877.
(39) Jorge, F. E.; Autschbach, J.; Ziegler, T. *Inorg. Chem.* **2003**, *42*, 8902–8910.
(40) Le Guennic, B.; Hieringer, W.; Gorling, A.; Autschbach, J. *J. Phys. Chem. A* **2005**, *109*, 4836–4846.
(41) Diedrich, C.; Grimme, S. *J. Phys. Chem. A* **2003**, *107*, 2524–2539.

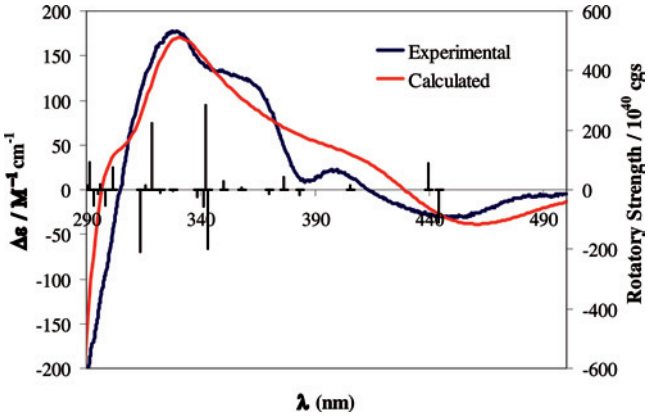

Figure 5. Measured (blue) and simulated (red) Λ geometry (B3LYP/LANL2DZ) CD spectrum of **5**. Rotatory strengths (black) for each transition are shown as unbroadened vertical lines.

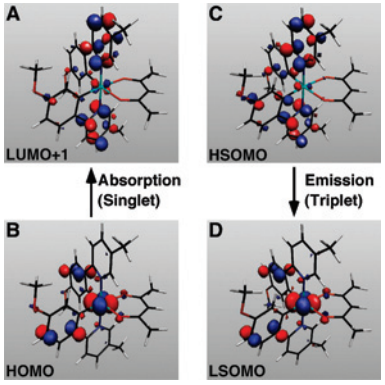

Figure 6. Orbitals of **5** associated with the absorption of a photon from the singlet ground state (B → A) and the emission of a photon from the triplet excited state (C → D). Both processes involve almost identical orbitals and parameters obtained from TD-DFT calculations of the singlet state and can be used as an approximation of this particular triplet−singlet transition (phosphorescence).

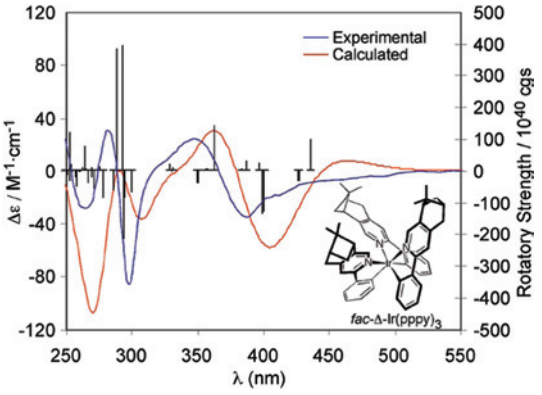

Figure 7. Measured (blue) and simulated (red) Δ geometry (B3LYP/LANL2DZ) CD spectrum of **fac-Δ-Ir(pppy)$_3$**.[16] Rotatory strengths (black) for each transition are shown as unbroadened vertical lines.

respect to the energies and relative strengths of the transitions; currently, no computational methodology exists to accurately predict the vibrational substructure of the spectrum, but it is clear that TD-DFT calculations at this level of theory can successfully assign the absolute configuration with reasonable confidence.[40,42] Our computational model

(42) Rinderspacher, B. C.; Schreiner, P. R. *J. Phys. Chem. A* **2004**, *108*, 2867–2870.

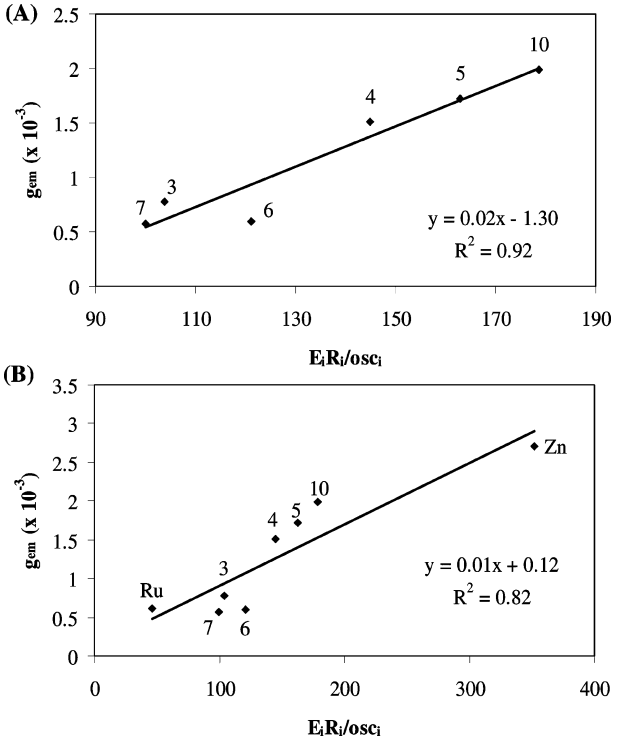

Figure 8. (A) Emission dissymmetry vs calculated E_iR_i/osc$_i$ for the Ir(III) complexes (**3**–**7**, **10**). (B) Emission dissymmetry (g_{em}) vs calculated E_iR_i/osc$_i$ including enantiopure Ru(II) and Zn(II) hemicage complexes (Figure 8).[15] See Table 3 for a summary of the individual values for each complex.

was, in fact, accurate at assigning this geometry, as verified by performing calculations on a previously published chiral complex of known configuration, fac-Δ-Ir(pppy)$_3$,[16] and comparing the spectrum to the experimentally measured CD (Figure 7).

2. Circularly Polarized Luminescence. The use of TD-DFT methods significantly decreases the computational cost required to accurately predict CD spectra; however, modeling CPL spectra is far more difficult. Calculations of emission spectra rely on recursions of normal modes that make predictions computationally unfeasible for all but the simplest molecules containing just a few heavy atoms. Our goal, therefore, was to develop a computational methodology that yields accurate approximations to experimental CPL spectra within reasonable computation time.

The first step in this process is the calculation of the absorptivity (ϵ) of the compound, which can be determined from the oscillator strength of the transitions involved (eq 4), where osc$_i$ is the oscillator strength of the ith transition:

$$\epsilon = \frac{2.174 \times 10^8}{\sigma} \sum_i^A \mathrm{osc}_i \, e^{-2.772\left[\frac{(\lambda - E_i)}{\sigma}\right]} \qquad (4)$$

For a given transition i, the absorption dissymmetry of the transition is defined by eq 5:

$$|g_{abs}(i)| = \frac{\Delta\epsilon}{\epsilon} \propto \frac{E_i R_i}{\mathrm{osc}_i} \qquad (5)$$

where R_i and osc$_i$ are the rotatory and oscillator strengths calculated for the singlet absorption transition and E_i is the energy of the absorption.

Table 3. Summary of Experimentally Measured Emission Dissymmetry Values and Calculated Data at the B3LYP/LANL2DZ Level

Complex	g_{em} ($\lambda_{1/2}$) × 10^{-3}	R_i (cgs)	osc$_i$	E_i (hartrees)	E_iR_i/osc$_i$
Λ-(ppy)$_2$Ir(acac) - **3**	+0.78	71.3486	0.0561	0.081513	103.67
Λ-(Fmppy)$_2$Ir(acac) - **4**	+1.51	86.3741	0.0551	0.092379	144.81
Λ-(MeOmppy)$_2$Ir(acac) - **5**	+1.72	107.8558	0.0567	0.085590	162.81
Λ-(Phmppy)$_2$Ir(acac) - **6**	+0.60	26.5894	0.0473	0.079982	44.96
Λ-(BrCyppy)$_2$Ir(acac) - **7**	+0.57	91.7900	0.0801	0.087211	99.94
Λ-Ir(FCyppy)$_3$- **10**	+1.99	116.3174	0.0645	0.099052	178.63
Λ-Zn(hemicage)[15]	+2.70	315.6177	0.0759	0.084666	352.07
Λ-Ru(hemicage)[15]	+0.61	82.9699	0.1359	0.075561	46.13

Because the geometry—and as a consequence the electronic structure—of the excited state should not change significantly during intersystem crossing from the singlet to the triplet state, the relaxation back to the ground state should thus possess equal magnitude oscillator and rotatory strength to that of the absorption transition, the latter of which is opposite in sign.[43] Thus, an emission dissymmetry value (g_{em}) can be extrapolated from the following relationship (eq 6):

$$|g_{em}(i)| \propto \frac{E_iR_i}{\mathrm{osc}_i} \tag{6}$$

with $E_i = E_{triplet} - E_{singlet}$ calculated at the triplet geometry.

Equation 6 was solved by initially optimizing the ground-state geometry using B3LYP/LANL2DZ with constraints of C_2 and C_3 symmetry for (C^N)$_2$Ir(acac) and Ir(C^N)$_3$ complexes, respectively. TD-DFT calculations were then performed at the optimized singlet-state geometry to obtain the rotatory (R_i) and oscillator (osc$_i$) strengths. The triplet geometry was optimized using unrestricted (open-shell) DFT calculations with the ground-state geometry as a starting point. Energies of the triplet and singlet states at the calculated triplet state geometry were obtained at the same level of theory. To ensure that the transitions chosen from the TD-DFT calculations were correct, the orbitals of the triplet highest singly occupied molecular orbital and the lowest singly occupied molecular orbital were compared to the orbitals involved for absorption, Figure 8.

Table 3 summarizes the determined experimental and calculated values, and Figure 8A shows excellent agreement between experiment and theory for the six resolvable Ir(III) complexes (**3**–**7**, and **10**). Furthermore, when ionic, enantiopure Zn(II) and Ru(II) hemicage complexes[15] (Figure 9) are included, the fit is less tight but still presents a strong correlation (Figure 8B), indicating that this trend holds true for a variety of complexes with diverse coordinated metals. The source of the reduction in effectiveness can be attributed to the poorer predictions of the energies (E_i) between the triplet and singlet states for different metal centers. Additionally, as can be seen from Figure 6B, the phenyl-substituted complex, **6**, deviates slightly in agreement with the other heteroleptic Ir(III) compounds. The discrepancy can be attributed to the greater flexibility provided by the additional phenyl ring, which leads to slight deviations in the excited-state geometry of the triplet state. Owing to the fact that our computational model requires that the excited triplet and singlet state geometries be the same, this flexibility leads to a breakdown in the prediction's effectiveness. Nevertheless, within the framework of structurally similar phosphorescent metal complexes, g_{em} can now be predicted extremely well. To our knowledge, this is the first example of an accurate prediction of g_{em}. Furthermore, this model can be extended to disparate metal complexes and thus provide a means of advance screening a wide variety of complexes for high dissymmetry values.

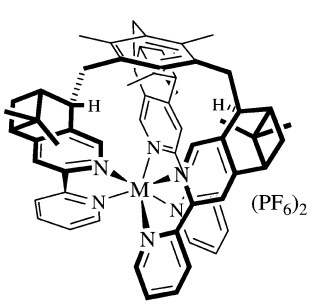

M = Ru(II), Zn(II)

Figure 9. Structure of hemicage complexes. M = Ru(II), Ru(hemicage); M = Zn(II), Zn(hemicage).

Conclusion

Herein, we have described the synthesis and characterization of a series of neutral iridium complexes and their enantiomeric resolution by chiral SFC, as verified by the characteristic mirror image motif in both the CD and CPL spectra. Emission dissymmetry values were measured for the series, all of which were on the order of 10^{-3}, with Ir(FCyppy)$_3$ (**10**) exhibiting the largest g_{em} value, 1.99 × 10^{-3}, for the iridium compounds. TD-DFT calculations were then applied to accurately predict the CD spectra of the resolved complexes. Subsequently, these calculations were expanded and applied to the emissive excited state in order to develop an unprecedented theoretical model capable of predicting emission dissymmetry. The calculation correlates extremely well to experimental measurements and can be generalized to other metals and ligand frameworks. Work is ongoing to better explain the relationship between substitution pattern and identity of the complexes to their chiroptical properties, with the ultimate goal of this research being the development of systems that optimize the emission preference of either right or left circularly polarized light.

Acknowledgment. This work was supported by the National Science Foundation (DMR-0605621 and CAREER Award No. CHE-0449755) and through a Camille and Henry

Dreyfus Foundation New Faculty Award. E.Z.-C. was supported by the Princeton Center for Complex Materials (PCCM) in the form of a postdoctoral fellowship. F.J.C. acknowledges support through a National Science Foundation Graduate Research Fellowship.

Supporting Information Available: The complete citation for ref 25 is included along with the CD and CPL spectra with corresponding calculated chiroptical predictions for **3**–**7** and **10**. This material is available via the internet at http://pubs.acs.org.

IC701747J

(43) Nakanishi, K.; Berova, N.; Woody, R. *Circular Dichroism: Principles and Applications*; VCH: New York, 2000; p 191.